JGISE Vol. 7 No. 2 (2024), pp. 103 - 114 | https://doi.org/10.22146/jgise.xxxxx

JGISE
Journal of Geospatial Information Science and Engineering
ISSN: 2623-1182 | https://jurnal.ugm.ac.id/jgise

Low-cost alternative flood modelling using CHIRPS data in the Way Garuntang Catchment, Bandar Lampung, Indonesia

Sahid Sahid, Yanto Putri Nana, Aziz Fahmi, Mardika Indra M Gilang, Asferizal Ferial, Zein Akbar Syukry, Diyaulhaq Wiedad, Yunida Devi

Institut Teknologi Sumatera, Indonesia

Penulis Korespondensi: Sahid Sahid | **Email:** sahid@pariwisata.itera.ac.id

Diterima (*Received*): 22/Feb/2024 Direvisi (*Revised*): 17/Dec/2024 Diterima untuk Publikasi (*Accepted*): 17/Dec/2024

ABSTRACT

Floods are hydro-meteorological events that could impact economic losses and threaten human life and it's categorized as the enormous disaster potential for global destruction. Floods occur because water overflows in potential areas due to exceeding the river's capacity. Flood modelling is the key in reducing the impact of losses resulting from flood disasters. Satellite-based rainfall data provides data with spatial and temporal distribution that has the potential to be an alternative as input in flood modelling. The availability of satellite rainfall data as input for flood modelling certainly requires an assessment of the modelling results' accuracy level. This research aims to investigate the performance of flood inundation modelling using CHIRPS data. The accuracy value of flood modelling results is calculated by comparing flood modelling results through Snyder-Alexejev synthetic unit hydrograph discharge calculations, which are then applied to 2D flood hydraulic modelling using HEC-RAS. The findings indicate that as an alternative to rainfall station data to model flood inundation, Chirps data have a level of accuracy that can be considered. Even though there are differences in the extent and depth of flood inundation between CHIRPS data and observation rainfall stations data, the results of modelling with CHIRPS data can contribute to mapping potential flood-prone areas.

Keywords: Satellite Rainfall Data, CHIRPS, Flood Modelling, 2D Flood Inundation Modelling

1. Introduction

Flood is a phenomenon characterized by the overflow of water beyond its capacity impacted by various factors such as intense precipitation, the ability of soil infiltration, the topographic condition, and land cover pattern within the water catchment region. Floods are classified as hydro-meteorological disasters with significant destructive potential on a global scale (Sarkar & Mondal, 2020). Rainfall events characterized by prolonged duration and heightened intensity have the potential to result in the overflow of water beyond the confines of rivers (Cheng et al., 2021). Moreover, another significant consideration is the soil's capacity for infiltration, which refers to its ability to absorb and accommodate the volume of water from precipitation (Hong et al., 2014). Digital Elevation Model (DEM) is a significant factor in determining the distribution of flood zones, as it represents the topographical conditions of the earth's surface (Sahid et al., 2018). According to the findings of the study, land-use change represent an additional contributing element to the occurrence of flooding, since they have the potential to diminish the discharge of surface water (Sushanth, K., & Bhardwaj, 2019).

A flood event poses a significant impact to human life and economic losses, hence classifying as a disaster. According to report from the National Agency of Disaster Risk Reduction (2021), Bandar Lampung City situated within the Lampung province determined as high disaster risk index which is one of the high hazard index is flood. According to data in 2022, Bandar Lampung has struck 29 flood disasters (BNPB, 2023). In addition, over 15 years from 2008 to 2022 Lampung province has significant infrastructure damaged about 12198 houses due to the flood impact, and approximately 2215 houses losses in Bandar Lampung, with the most severe occurred in 2008 impacted to 1234 houses (BNPB, 2023). In addition to the physical

destruction to infrastructure, flood catastrophes can also have enduring impacts on both physical and psychological well-being, including post-traumatic conditions (A. K. Carra, 2017; Fernandez et al., 2015; Stephenson et al., 2014).

Given the significant ramifications associated with flood calamities, it is imperative to undertake flood hazard modelling as a means of mitigating the risks involved. This approach facilitates the identification of areas susceptible to flooding. The outcomes of this modelling endeavor can be effectively employed to establish flood hazard zoning, which in turn can be utilized for the purposes of mitigating potential risks, issuing early evacuation alerts, identifying secure flood-prone areas, and enhancing community preparedness and response mechanisms in the face of flood incidents (B. K. Singh, 2014; Zope et al., 2016; Pratiwi & Santosa, 2021). Numerous academics have conducted flood hazard modelling utilizing the integration of Remote Sensing (RS) technologies with Geographic Information Systems (GIS). The study conducted by Hiệu et al., (2013) employed SPOT 6 Satellite Imagery in a temporal resolution to ascertain flood inundation zones by examining the visual changes that occurred prior and after to the flood event. Various study also conducted to simulate the flood inundation utilized two dimensions (2D) model, it achieved through the integration of hydraulic modelling with Geographic Information Systems (GIS) (Brunner et al., 2015; Khattak et al., 2016; Parsa et al., 2013; Vozinaki et al., 2017).

The primary input for flood modelling is precipitation data. Generally, the main source of the precipitation data used for flood modelling are observational rainfall data from rainfall station (Cheng et al., 2021; Islam, 2020; Sarkar & Mondal, 2020; Santosa et al., 2010). The requirement for extended-duration rain data and spatial distribution rainfall station its associated high costs can be attributed to the implementation of Government Regulation Number 47 of 2018, which pertains to the categorization and tariffs for non-tax state revenue types applicable to the Meteorology, Climatology, and Geophysics Agency (BMKG), as well as the provision of observation stations across various regions. The primary challenge in modelling flood hazard is precipitation detailed to daily rainfall data. In order to face the challenge due to the observational rain data from rainfall station, satellite-derived precipitation data can serve as a viable alternative. Numerous scholars have conducted comparative analyses on the dependability of satellite-derived precipitation data in relation to observed precipitation data. Ramly et al., (2020) conducted flood modelling simulation by utilizing rainfall data obtained from RAIN RATE AUTO V2. The result shows favorable outcomes with error percentages that were deemed acceptable. The utilization of rain intensity data derived from satellite sources enables the comparison of flood simulation outcomes and hydrographs obtained from flood occurrences, as demonstrated in previous studies (Ozkaya & Akyurek, 2019; Yucel, 2015). The reliability of rain data derived from the GSMaP, TRMM, GPM, and PERSIANN satellites is comparable to that of observational rain data (Asferizal, 2022).

The utilization of Climate Hazards Group InfraRed Precipitation with Station (CHIRPS) rainfall data as an alternate input data for flood modelling still needs to be improved. Limited data access and the sparse availability of rainfall data from conventional rainfall stations highlight CHIRPS rain data as a viable alternative input for flood inundation modelling. Using satellite rainfall data has successfully addressed issues related to regional coverage and data completeness in flood modelling. This research aims to investigate the accuracy of flood modelling results obtained through hydraulic modelling techniques using a combination of HEC-RAS and GIS applications utilizing CHIRPS rainfall data. The assessment focuses on the comparison of two rainfall source data, namely from CHIRPS and rainfall station over Way Garuntang watershed.

2. Data and Methods

2.1. Study Area

The study is located within the geographic coordinates of 5° 19' 21.34"S to 5° 31' 10.61"S and 105° 10' 29.93"E to 105° 21' 9.23"E, specifically located in the Way Halim sub-district, Bandar Lampung City (Figure 1). The sub-district has been identified as the region with the highest flooding incidents in Bandar Lampung City. Notably, in 2022, it accounted for 6 out of 29 flood events in the Way Halim (BNPB, 2023). Also, the sub-district has been categorized as having the highest population density and primarily classified by residential land use. Hydrologically, The Balau River, which serves as the primary river within the Way Garuntang watershed in Bandar Lampung City, traverses along this location. The precipitation levels in this region exhibit a significant increase throughout the period spanning from November to May. The circumstance amplifies the susceptibility to floods inside the Way Halim sub-district. The circumstances contribute to the heightened susceptibility of Way Halim District to flooding. A large population density in the area may increase the likelihood of significant losses due to flood events. The hydrological response area to calculate the flood discharge is located in the upper part of the Way Garuntang Watershed within the total area calculated approximately 15.37 km2. Furthermore, flood modelling location was applied along the Way Balau River with a total length of about 4.06 km.

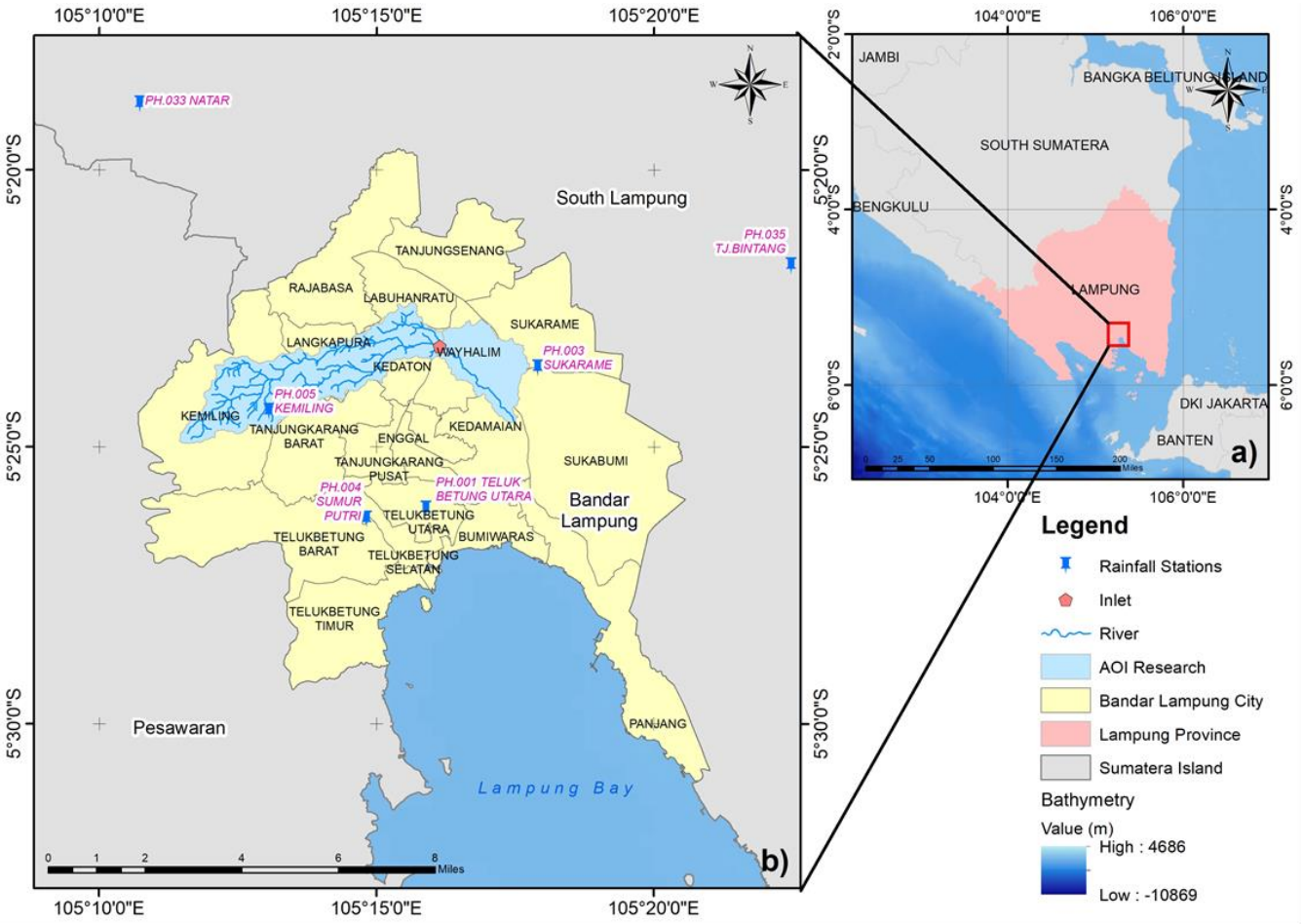

Figure 1 Image a) shows the research location positioning on Sumatra Island area marked with a red box which is the Lampung province, while image b) depicts the research location in Way Garuntang watershed marked with red rectangle color

2.2. Data and Methodology

2.2.1. Regional Rainfall Analysis

The analysis of regional rainfall is employed to ascertain temporal and spatial rainfall trends within the hydrological response area located in the upstream Way Garuntang watershed. The research entails the computation of the maximum regional average precipitation by utilizing maximum daily rainfall data obtained from both rainfall observation stations and daily CHIRPS data. Before analyzing rainfall data from rainfall stations and CHIRPS, the data authenticity test is conducted using a double mass curve to ensure the quality of rainfall data from the stations. Subsequently, CHRISP data is evaluated through bias correction analysis, involving the calculation of correction factors by comparing CHIRPS rainfall data with data from the rain stations. Once both types of data are confirmed to be of good quality, the isohyet method is calculated by considering the topography of the study region, rendering it more comprehensive compared to alternative approaches as it integrates both the spatial distribution of rain stations and the topographic characteristics in delineating the borders of the precipitation zone. The findings are quantified in millimeters (mm) concerning daily precipitation. The counter line isohyet analysed using ArcGIS software within the spatial analysis tool.

2.2.2. Runoff Coefficient Analysis

The Cook coefficient analysis is employed to ascertain the C value within the hydrological response area. The analysis for determining the C value involves considering four key elements: relief (slope), vegetation cover, soil infiltration, and river flow density (Meyerink, A, 1970). Another study implies that Cook's analysis could estimate peak flows considering four categories of numerical values and weights of attributes namely: terrain, infiltration, vegetation cover, and storage conditions (Santos et al., 2017). This study utilized classification of Cook coefficient conducted using Geographic Information System (GIS) operations. This involves overlaying each element layer, as illustrated in Table 1.

2.2.3. Return Period Rainfall Analysis

A sequence of statistical analysis steps, including frequency analysis, the Chi-Square statistical test, and the Smirnov-Kolmogorov test, was undertaken to identify the type of frequency distribution that meets the criteria given the input conditions of maximum

regional rainfall data. Determining the distribution type is crucial for estimating the maximum design rainfall based on the statistical characteristics of the available data. Frequency analysis hinges on establishing the probability of future rainfall magnitudes by relying on the statistical properties of the acquired data (Harto, 1993). Return periods for maximum design rainfall were computed in this study for intervals of 2, 5, 10, 20, 50, and 100 years. These return periods' calculation is a basis for assessing potential future hazards (Yucel, 2015) and are fundamental aspect of the planning process (Cannon et al., 2015).

Before utilizing the results of annual return period calculations as input for flood discharge hydrograph computations, a preliminary estimation of effective design rainfall is conducted for each return period. The calculation of effective rainfall aims to exclude the portion of rainfall not contributing to surface runoff. The effective rainfall value is derived from the computation of return periods for maximum rainfall, incorporating coefficient values obtained from the Cook coefficient (C) calculations for each return period. Additionally, since rainfall data used in flood hydrograph calculations must be in hourly units, the data representing effective maximum rainfall periods is converted into hourly rainfall using the Mononobe method for each return period. Notably, the typical rainfall duration in the Indonesian region is approximately 5-7 hours per day (Sarido et al., 2008). Consequently, in this study, the return periods of rainfall are transformed into hourly rainfall for 6 hours.

Table 1 Cook Coefficient Classification

Watershed characteristics	**Characteristics of Runoff Results**			
	Extreme Value 100	**High 75**	**Normal 50**	**Low 25**
Relief/Slope	(40) Very steep with a general slope condition >30%	(30) Hilly terrain with an average slope of 10% - 30%	(20) Undulating terrain with an average slope of 5% - 10%	(10) Relatively flat area with an average slope of 0% - 5%
Soil Infiltration	(20) Open ground with no covering, whether it be rocks or a thin layer of soil; infiltration capacity is disregarded	(15) Low infiltration rate, having clay soil texture or other soil types with low infiltration capacity	(10) Normal, loam soil texture, infiltration type is nearly the same as grassland soil type	(5) High, majority of the soil has a sandy texture or other types of soil that quickly absorb water.
Land Cover	(20) Bare ground or very sparse vegetation.	(15) Sparse natural land cover, buildings, and plants, less than 10%; poor drainage conditions	(10) Well-covered with vegetation, grass, woody plants, or vegetation cover not more than 50%, uncovered	(5) Dense vegetation cover, approximately 90% of the area is covered by vegetation, including both grass and woody plants
River Density	(20) High, high surface depression or Channel Density >5 channels/km^2	(15) Normal, having surface depressions such as lakes, reservoirs, or marshes <2% of the drainage area; Channel Density 2 - 5 channels/km^2.	(10) Low, has a well-developed drainage system or Channel Density <2 channels/km^2	(5) Neglected, surface depressions are few and shallow, drainage is poor and minimal

Source: Adapted from Meyerink, A, (1970), Santos et al., (2017), and Sahid, (2024)

2.2.4. Synthetic Unit Hydrograph

Hydrograph analysis is necessary to determine rainfall distribution over time and calculate peak discharge. Data limitations in locations without actual discharge measurements necessitate using synthetic unit hydrographs (SUH) to establish the flow hydrograph. SUH is a method applicable for determining the flow hydrograph in locations lacking discharge measurements (Wilkerson & Merwade, 2010). The Snyder SUH method is widely employed to determine flow hydrographs. Snyder SUH establishes empirical relationships between watershed characteristics, such as area (A) (km^2), main river length (L) (km), distance from the outlet to the calculated gravity point of the region (Lc), and three other parameters, including time lag (h), peak discharge (Qp) (m^3/s), and base time (tb) (P. K. Singh et al., 2014; Snyder, 1938). Snyder, (1938) conducted a study in the Appalachian Mountains with watershed areas ranging from 10 to 10,000 square miles (26 – 259,000 km^2) in the United States. The use of the Snyder SUH method is widespread in several countries, including Indonesia, and some studies indicate that hydrograph analysis results closely approximate actual discharge hydrographs (Prasad & Pani, 2017; Thapa & Wijesekera, 2017).

2.2.5 Two-Dimensional Flood Inundation Modelling

Flood inundation modelling is conducted using hydraulic analysis applied through HEC-RAS software

and its RAS Mapper to delineate the extent of flood inundation spatially. Land use information obtained from the Agency for Regional Development Bandar Lampung City is utilized to derive Manning's roughness coefficient values, a prerequisite for using HEC-RAS software for flood modelling. Land use data is also employed to obtain Manning's roughness coefficient values, another prerequisite for using HEC-RAS software in flood modelling. HEC-RAS offers various features that facilitate hydrological studies, including hydrological factors, geometric data correction, river profile (cross-section) editing, Manning coefficients editing, and the capabilities of its RAS Mapper (Deniz et al., 2017).

2.2.5. Flood Modelling Quality Assessment

Validating flood inundation resulting from modelling is crucial for evaluating the accuracy of the modelling outcomes. Flood maps and field survey findings are crucial in this validation process (Venus, 2015). Flood event maps are obtained from the Agency for Regional Development in Bandar Lampung City, and data points for flood incidents gathered through on-site surveys are utilized to assess the model outcomes. The purposive sampling technique collects field observation samples to identify measurement locations for past flood events. The selection of measurement locations is based on areas around the Way Garuntang River that have experienced flooding. The accuracy test comparison of modelling results involves evaluating flood depth and areal distribution from both types of input data (Rainfall station and CHIRPS). Accuracy tests are calculated using Root Mean Square Error (RMSE) and Mean Absolute Error (MAE) values. The percentage of accurate flood inundation locations from the modelling results is assessed by comparing the inundated pixel values with existing field conditions, determining whether the sampled locations have experienced flooding. Initially assigned a value of 1 before the survey to indicate inundation, the number of sampling locations is adjusted to 0 after the survey if the pixel location has never experienced flooding. Consequently, the results of flood event location evaluation ascertain the accuracy of flood inundation distribution locations from the modelling results.

3. Results And Discussion

3.1. Hydrological Analysis

Rain data sourced from observation rain posts needs to be assessed for data consistency. The results of checking the continuity of rain data show that there are 2 rainfall stations, namely the Sukarame from 2009 to 2012 and the Sumur Putri from 2009 to 2011 whose rainfall station data results are missing. Filling the missing rain data is done by using the inverse square distance method by considering surrounding precipitation value from rainfall station and measuring the distance in approaching the missing precipitation value. The double mass curve test has been tested to validate the quality of the precipitation data and there is no data discrepancy so that rain data can be used in regional rainfall analysis.

Furthermore, the evaluation results show that CHIRPS data in estimating daily maximum rain when compared to the daily maximum rain data from the rainfall station is underestimated, around 74.44% shows the maximum rain value below the observation rain value. Then, to overcome the underestimates, it is necessary to calculate the correction bias of the CHIRPS data. The selection of the best type of correction method is done by looking at the RMSE value and the Nash Sutcliffe Efficiency test (NSE) which is the most compared to the results of each method, namely the Piani, Linear Scaling, and Quantile Mapping (QMap) methods. The suitable bias correction results show that the linear scaling method is the closest method with an RMSE value of 21.45 and an NSE value of 0.09 (Table 2).

Table 2 Comparison of the results of using bias correction methods on CHIRPS rain data

Bias Correction Method	RMSE (mm)	NSE
Piani	30.5	-0.85
Linear Scaling	21.45	0.09
Qmap_PTF	46.55	-0.8
Qmap_QUANT	46.98	-0.84
Qmap_RQUANT	46.65	-0.81
CHIRPS Original data	28.18	-0.58

Furthermore, regional rainfall analysis is carried out with data sources derived from observation rain posts and CHIRPS data. The calculation of regional rainfall is carried out in the hydrological response area located in the upstream area with an area approximately 15.37 km^2 (Figure 2). The maximum precipitation data sourced from both rainfall station and CHIRPS data are used as input in interpolation for regional rainfall analysis. The results of the interpolation analysis are in the form of isohyet grid data which are then derived to obtain isoline contours. Isoline contours are imaginer lines connecting high rain points at each rainfall station. The isoline is made with a contour interval of 5 mm with the assumption that making a tight contour interval can produce rainfall areas that are close to field conditions.

The results of the regional rainfall analysis over a span of 15 years from 2008 to 2022 in the study area show that the maximum value of regional rainfall is 157.12 mm, with an average value of 108.48 mm. The highest rainfall occurred in 2010. While the minimum value of regional rainfall occurred in 2012 with a regional rainfall value of 54.03 mm (Figure 2). The results of the regional rainfall analysis with the source of corrected CHIRPS rain data show that the maximum value of regional rainfall occurred in 2016 with a total value of 140.88 mm, while the average and lowest values were 86.63 mm and 42.95 mm (Figure 2). The

analysis of rainfall data for the region, utilizing information from rain gauge stations and CHIRPS, reveals variations in both the quantity and timing of peak rainfall values. The difference in maximum regional rainfall values between the two datasets is 16.24 mm, representing a disparity of 10.34%. Moreover, there is a temporal shift in the occurrence of maximum regional rainfall values from 2010 to 2016 (Figure 2). These noted distinctions may necessitate additional analysis to explore factors contributing to the disparities in the data results.

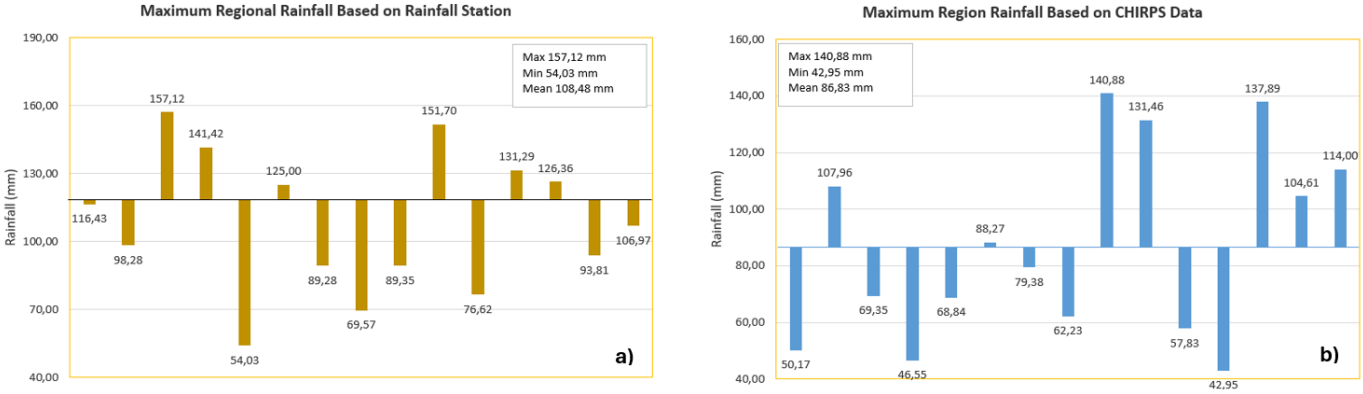

Figure 2 Rainfall calculation of the study area from 2008 - 2022, a) use of rainfall data of observation post, b) CHIRPS rainfall data

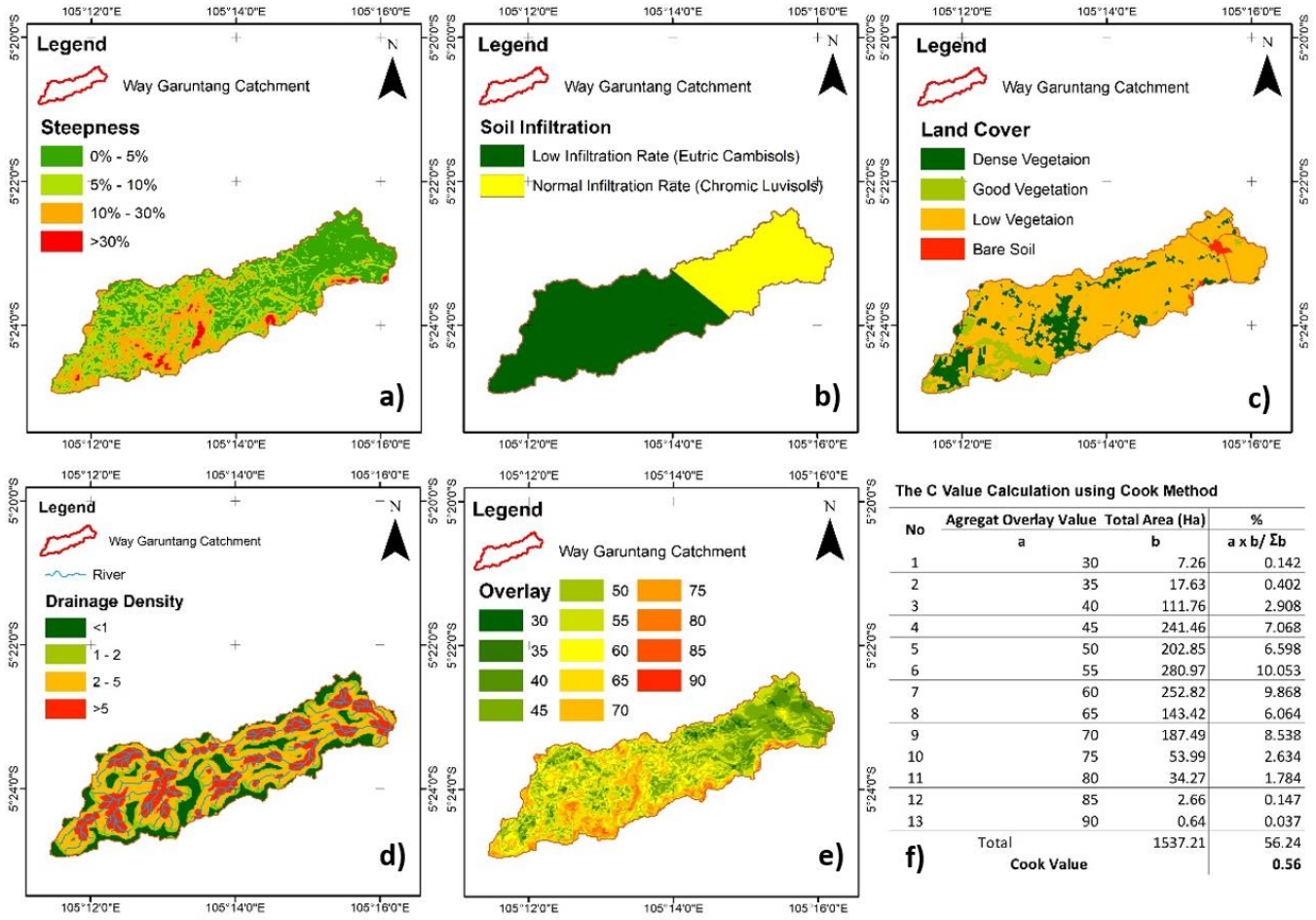

The C Value Calculation using Cook Method

No	Agregat Overlay Value a	Total Area (Ha) b	% a x b/ Σb
1	30	7.26	0.142
2	35	17.63	0.402
3	40	111.76	2.908
4	45	241.46	7.068
5	50	202.85	6.598
6	55	280.97	10.053
7	60	252.82	9.868
8	65	143.42	6.064
9	70	187.49	8.538
10	75	53.99	2.634
11	80	34.27	1.784
12	85	2.66	0.147
13	90	0.64	0.037
	Total	1537.21	56.24
	Cook Value		0.56

f)

Figure 3 Calculation of runoff coefficient value using Cook method, a) Relief or slope condition, b) soil type condition, c) land cover condition, d) river flow density condition, e) cook value overlay result, f) cook value calculation table

3.2. Runoff Coefficient Analysis

Runoff coefficient is estimated using the Cook method considering the four parameters namely relief (slope conditions), soil infiltration, land-cover, and drainage density over the hydrologic response area. The relief aspect of the location with low slope conditions with a range of 0% - 5% or flat with a percentage of 40.47% are assumed to have runoff characteristics. Slightly steep slopes are found in the southern part of the hydrological input area with a percentage of 2% of the total area. The land cover condition of the study area is classified into 4 land cover classes with the largest percentage of 74.50% is the type of natural vegetation land cover that rarely shows the condition of the water rate during rainfall will immediately flow. Calculation of drainage density is calculated based on river density analysis which results in that the hydrological input area of the study has the following 4 flow density classes namely very low, low, normal, and high (Figure 3d). The normal flow density class dominates the area with a total percentage of 43.27%. The normal flow density class means that there are 1 - 2 streams per km^2.

Moreover, the assessment of infiltration rate considering the soil conditions to estimate the ability of soil to infiltrate water (Figure 3b). The soil types found in the hydrological input area are divided into 2 types, namely Chromic Luvisols and Eutric Cambisols. The Chromic Luvisols soil type is assumed to have a normal infiltration rate because this soil type is a soil containing loam, while the Eutric Cambisols soil type has a low infiltration capability category because this soil type has a clay texture. Based on the results of the calculation of the C value, the total runoff coefficient value is 56.24 or 0.56 which is a type of Normal class (Figure 3f), then the flow coefficient of the hydrological input area is 0.56 which indicates that about 56% of the falling rainfall will be converted into surface flow and vice versa. The stages of calculating the C value using the cook method can be seen in Figure 3.

3.3. Return Period Rainfall Analysis

The return period rainfall analysis is carried out by first determining the type of rain frequency based on the rain distribution method. The results of the design rainfall calculation with the data source of the observation rain post show that the return period for 2 years produces a rainfall amount of 107.41 mm, 5 years of 135.07 mm, 10 years of 149.84 mm, 20 years of 161.98 mm, 50 years of 175.40 mm, and for the 100-year return period of 184.13 mm (Figure 4). The effective design rainfall value in each period is the rainfall value that has received consideration of the amount of rainfall that becomes runoff or runoff compared to the runoff coefficient value. The results of the comparison of the hourly rain distribution show that the rain data sourced from the observation rain post in the 2-year return period is greater than the CHIRPS rain data, but the higher the return period, namely in the annual return period, the number of CHIRPS hourly rain distribution data is greater than the rain data sourced from the observation rain post.

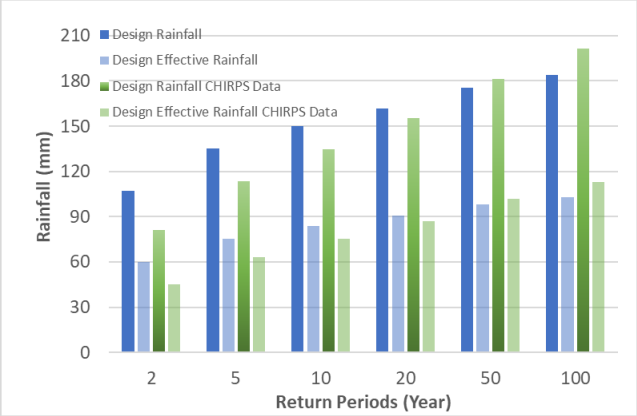

Figure 4 Comparison of Design precipitation Values for Each Return Period and Effective Design precipitation using rainfall station data and CHIRPS

3.4. Flood Synthetic Unit Hydrograph (SUH) Analysis

The results of the SUH Snyder-Alexejev calculation found that the time required for water to flow (*tp*) due to rain falling to reach the end point or outlet is about 3.88 hours and the time required between the onset of rain to reach the peak of the hydrograph is about 4.38 hours. Based on the results of making superposition hydrographs on a 2-year return period, the time to reach peak discharge is 7 hours.

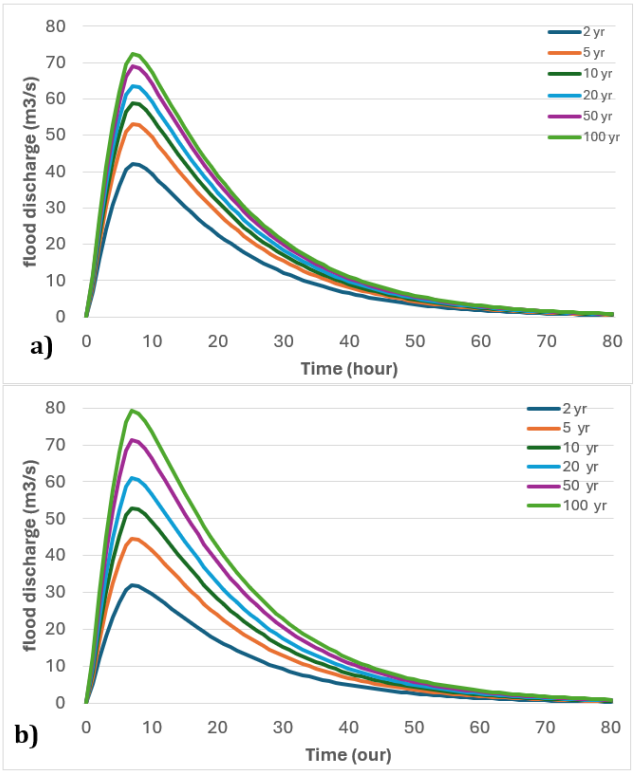

Figure 5 Design Rainfall Distribution with Superposition Hydrograph of each return period, 2-year return period, 5-year return period, 10-year return period, 20-year return period, period 50-year return

period, and 100-year return period, a) observed rainfall post data, b) CHIRPS rainfall data

The results of the analysis of the amount of peak discharge with data sources derived from the observation rain post at each return period of 2, 5, 10, 20, 50, 100 years amounting to 42.21 m^3/s, 53.08 m^3/s, 58.88 m^3/s, 63.65 m^3/s, 68.92 m^3/s, 72.36 m^3/s respectively (Figure 5a). Furthermore, the results of the analysis of the peak discharge amount with data sources derived from CHIRPS at each return period of 2, 5, 10, 20, 50, 100 years amounted to 31.84 m^3/s, 44.53 m^3/s, 52.92 m^3/s, 60.95 m^3/s, 71.34 m^3/s, 79.18 m^3/s sequentially (Figure 5b).

3.5. Two-dimensional (2D) Flood Inundation Modelling

Two-dimensional (2D) flood inundation modelling was carried out on a 4.06 km long river to derive inundation distribution due to water runoff from Way Halim River. The results of flood modelling are in the form of raster data with pixel values containing flood depth values. The results of flood modelling at each return period using SUH data sourced from the processing of observation post data show differences in area at each return period (Figure 6a). The average difference in flood inundation at the return periods of 2, 5, 10, 20, 50, and 100 years is 5.57 ha. The area of flood inundation modelling results sourced from SUH input data processed from CHIRPS data shows a difference in area at each return period which is increasingly widespread in line with the increase in the return period of the flood (Figure 6c). The average difference total area of flood inundation modelling results using CHIRPS rainfall data is 8.43 ha. The highest difference in area occurs in the 2-year flood return period with a total area difference of 11.80 ha. The results of the calculation of the area difference in the 50 and 100 year return periods show that the flood area is smaller than the flood area modeled with CHIRPS input data. The difference in the distribution of flood inundation area when viewed spatially can be involved in the difference in inundation area in the middle to downstream of the modelling (**Figure 7**).

In addition to the difference in inundation area, the difference in flood inundation height of the modelling comparison results shows that there is a difference in the maximum height of flood inundation both using input data derived from observation rainfall posts and CHIRPS data. The average difference in the height of flood inundation with input data from the observation rain post at each flood return period is 0.40 m, while the modelling results with CHIRPS rain data input show the difference in the maximum inundation height at each return period of 0.65 m (Figure 6b). The spatial distribution of differences in flood inundation height values from flood modelling derived from observed rainfall post data and CHIRPS data shows an increase in height differences downstream for the 2-year to 20-year flood period (Figure 8). In contrast, the 50-year and 100-year flood return periods show that the difference in elevation value is getting bigger towards the downstream (Figure 6d).

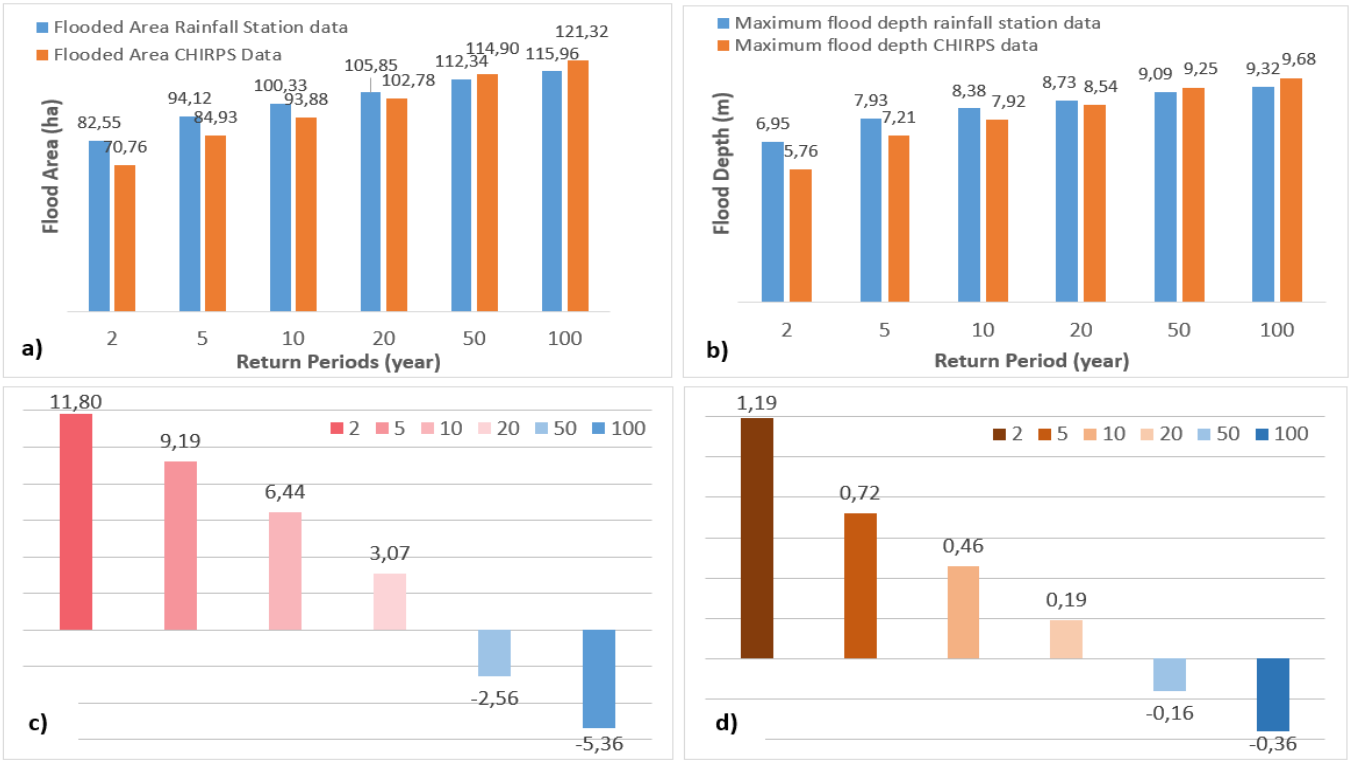

Figure 6 Flood inundation area modelling results with SUH data sourced from rainfall station and CHIRPS data, a) the comparison flooded area, b) the difference maximum flood depth, c) the difference flooded area (ha), and d) the difference maximum flood depth (m)

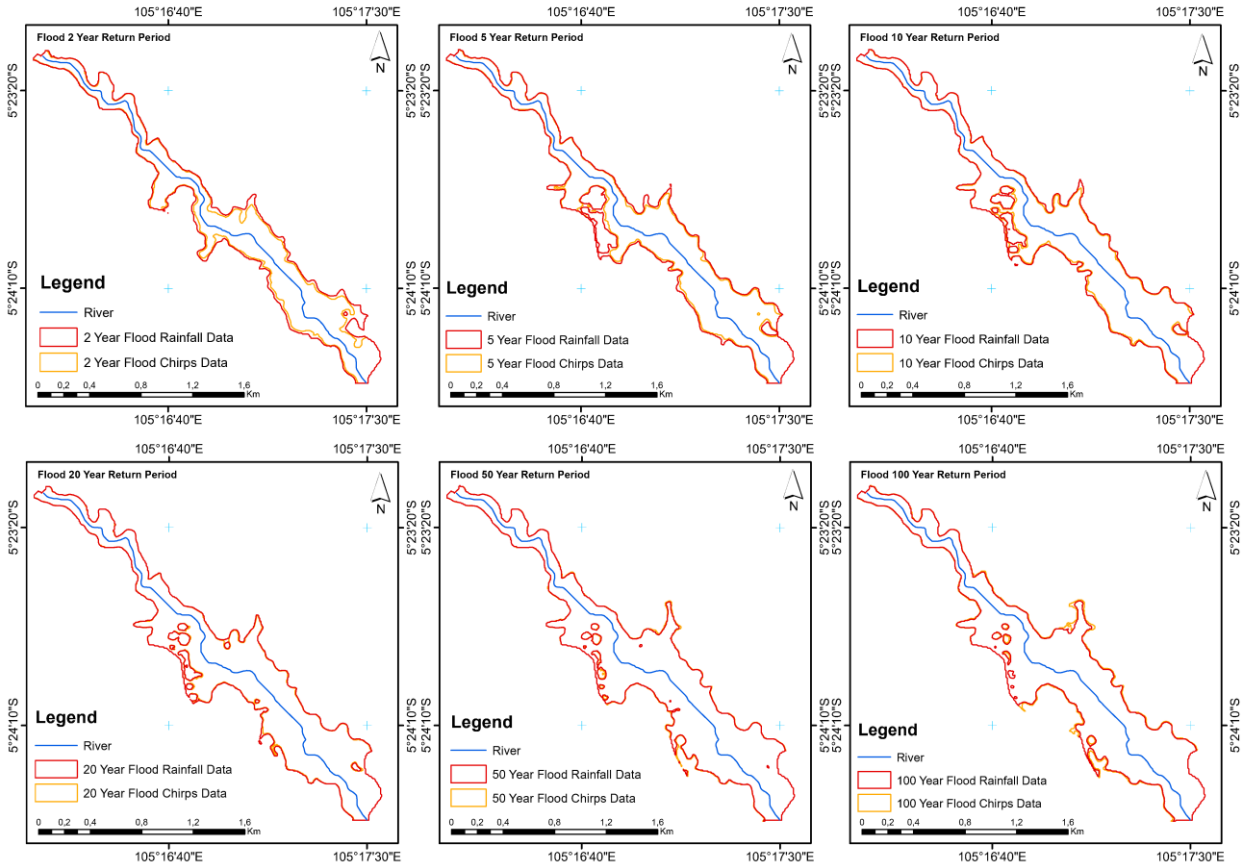

Figure 7 Comparison of flood inundation distribution for each return period between rainfall station and CHIRPS data

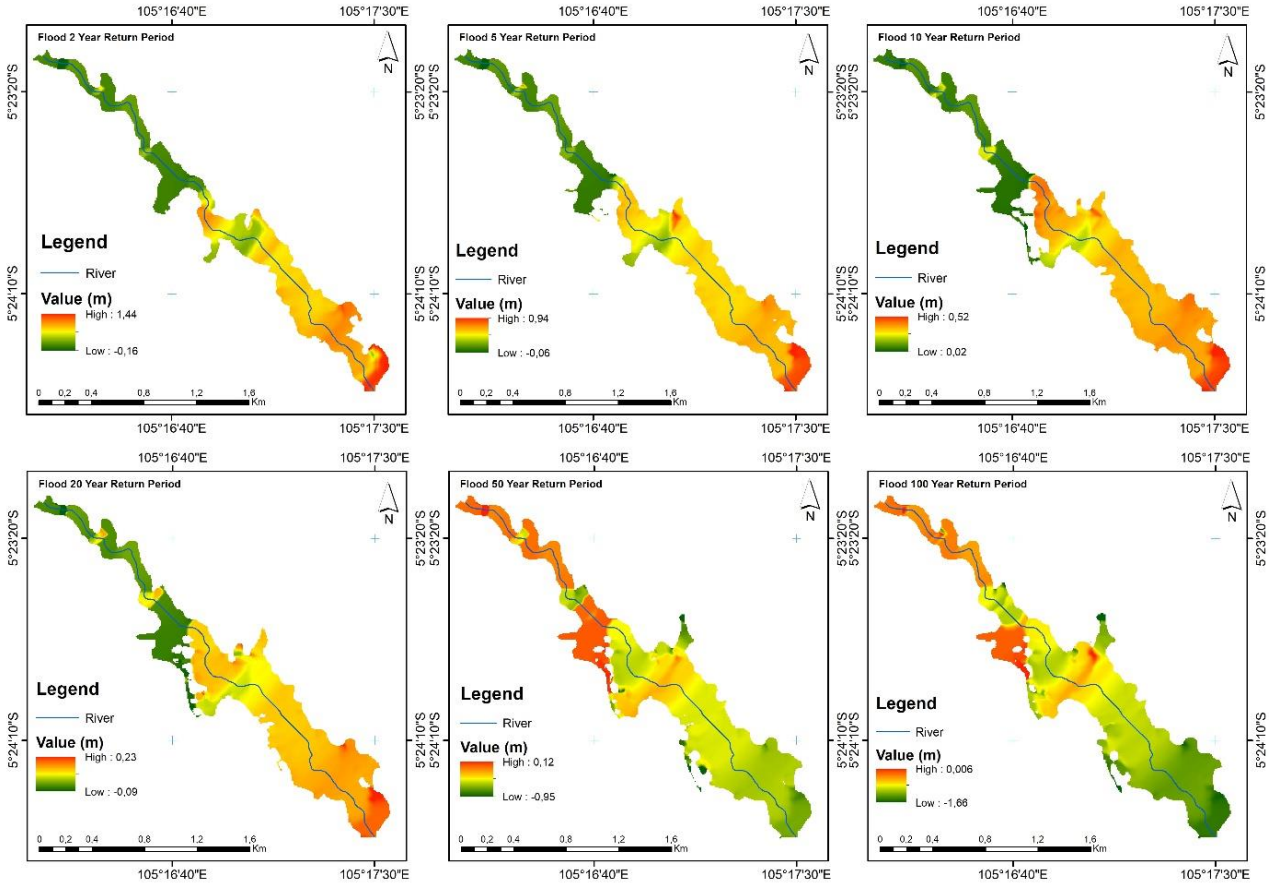

Figure 8 Difference in Flood Inundation Elevation Values between Observation Rain Post data input and CHIRPS Data

3.6. Flood Inundation Model Validation

Model accuracy validation was conducted to evaluate the resulting flood inundation model, utilizing data from rainfall stations and CHRIPS. A total of 54 model validation points were employed to validate the outcomes of flood inundation modelling. Accuracy testing involved calculating RMSE and MAE values on observed rainfall stations and CHIRPS data at field observation locations, which were subsequently compared to assess differences between the two datasets. Model validation results revealed variations in flood inundation heights from rainfall stations and CHRIPS data in each recurrence interval. The accuracy test results for flood inundation heights in each recurrence interval indicated that the average RMSE and MAE for observed rainfall station data were 2.56 m and 2.19 m, respectively. In comparison, the average RMSE and MAE for CHIRPS data were 2.43 m and 2.06 m respectively. Based on these differences, it was determined that the accuracy of flood inundation height modelling using CHIRPS was superior, with an improvement of 5.16%.

Moreover, the accuracy of flood modelling results was assessed by comparing the raster modelling results with existing conditions. The assessment results demonstrated that flood inundation modelling using CHIRPS data achieved a higher accuracy level, reaching 74.22%, compared to modelling results using observed rainfall station data. This evaluation provides an overview indicating that modelling with CHIRPS input data is more precise in predicting inundated areas compared to modelling using observed rainfall station data.

In the context of flood inundation modelling, selecting Digital Elevation Model (DEM) data is critical for obtaining accurate results. DEMNAS data, a Digital Surface Model (DSM) data provides information about the height of land cover, including vegetation and buildings, as well as the original ground height without any cover on top of it (Danoedoro et al., 2022). Thus, when modelling floods using DSM data, the resulting flood heights will be based on surface elevation rather than the actual ground elevation. A sensitivity assessment of the DEM is also necessary to ensure that the elevation data used aligns with the requirements, thereby achieving a high level of accuracy in flood modelling (Sahid et al., 2024). The more detailed the topographic data used, the better the accuracy of the results, as topographic data is a pivotal factor in flood modelling (Casas et al., 2006). Despite significant differences in height results, CHIRPS data can be considered an alternative in flood inundation modelling to map locations with potential flood occurrences.

4. Conclusion

Floods are hydro-meteorological disasters that can cause economic losses and threaten human life. Flood inundation modelling could be the first step to reduce the impact of flood losses. Satellite-based rainfall data, such as CHIRPS, has potential as input for flood modelling. However, it is necessary to correct the bias in the CHIRPS data to approach the observed rain data. The first stage of analysis is hydrological analysis which includes rain data quality test, CHIRPS rain data accuracy test, regional rainfall analysis, runoff coefficient analysis, and design rainfall analysis. Then 2D modelling of flood inundation was carried out using HEC-RAS. The results of the modelling show the difference in the extent and height of flood inundation between input data from observation posts and CHIRPS. This difference tends to increase as the flood return period increases.

Furthermore, it is necessary to continue to monitor and improve CHIRPS satellite rainfall data for better use in flood inundation modelling. Further research is needed to understand and address the accuracy in flood inundation modelling results between observed rainfall data and CHIRPS. The results of flood inundation modelling can be used for flood risk mitigation and management planning, as well as to identify flood-prone areas. Flood risk reduction efforts, such as the construction of levees or more efficient waterways, can be made based on the results of this flood inundation modelling.

5. Conflict of Interest

The authors declare no competing interest.

6. Acknowledgment

We acknowledge the support received from the Balai Besar Wilayah Sungai Mesuji Sekampung, specifically for providing the "SHARE: rainfall data over the research location." Funding acknowledgment is extended to the Institut Teknologi Sumatera (ITERA) for providing the research grant 631be/IT9.2.1/PT.01.03/2023 through “Hibah Penelitian ITERA 2023”, and we are grateful to the Regional Disaster Mitigation Agency of Bandar Lampung for supplying the necessary observation datasets crucial for this study. Our sincere thanks go to anonymous reviewers for their constructive comments that have significantly enhanced the quality of our manuscript. Additionally, we would like to express our special gratitude to the providers of the utilized products, the Climate Hazards Group InfraRed Precipitation with Station (CHIRPS) from the Climate Hazards Group at the University of California, Santa Barbara.

7. References

A. K. Carra, M. C. (2017). Posttraumatic Growth Among Australian Farming Women After a Flood After a Flood. *Journal of Loss and Trauma*. https://doi.org/https://doi.org/10.1080/15325024.2017.1310506

Asferizal, F. (2022). Analisis Perbandingan Kehandalan Data Hujan GSMaP, TRMM, GPM dan PERSIANN

Terhadap Data Obsevasi Dalam Rentang Waktu Penelitian 2020-2021. *Journal of Infrastructure Planning, and Design*, *2*(1), 33–41.
Badan Nasional Penanggulangan Bencana. (2024). *Data Kejadian Bencana*. https://gis.bnpb.go.id
BNPB. (2021). *Indeks Risiko Bencana Indonesia (IRBI) Tahun 2021*. https://inarisk.bnpb.go.id
BNPB. (2023). *Data Kejadian Bencana Banjir*. Badan Nasional Penanggulangan Bencana. https://dibi.bnpb.go.id
Brunner, G. W., Wre, D., Piper, S. S., Jensen, M. R., & Chacon, B. (2015). Combined 1D and 2D Hydraulic Modeling within HEC-RAS Two-Dimensional Modeling Capabilities. *World Environmental and Water Resources Congress 2015*, 1432–1443.
Cannon, A. J., Sobie, S. R., & Murdock, T. Q. (2015). Bias correction of GCM precipitation by quantile mapping: How well do methods preserve changes in quantiles and extremes? *Journal of Climate*, *28*(17), 6938–6959. https://doi.org/10.1175/JCLI-D-14-00754.1
Casas, A., Benito, G., Thorndycraft, V. R., & Rico, M. (2006). The topographic data source of digital terrain models as a key element in the accuracy of hydraulic flood modelling. *Earth Surface Processes and Landforms*, *31*, 444–456. https://doi.org/10.1002/esp.1278
Cheng, Y., Sang, Y., Wang, Z., Guo, Y., & Tang, Y. (2021). Effects of Rainfall and Underlying Surface on Flood Recession—The Upper Huaihe River Basin Case. *International Journal of Disaster Risk Science*, *12*(1), 111–120. https://doi.org/10.1007/s13753-020-00310-w
Danoedoro, P., Gupita, D. D., Afwani, M. Z., Hadi, H. A., & Mahendra, W. K. (2022). Preliminary Study on the Use of Digital Surface Models for Estimating Vegetation Cover Density in Mountainous Area. *Indonesian Journal of Geography*, *54*(3), 333–343. https://doi.org/10.22146/ijg.60659
Deniz, D., Arneson, E. E., Liel, A. B., Dashti, S., & Javernick-Will, A. N. (2017). Flood loss models for residential buildings, based on the 2013 Colorado floods. *Natural Hazards*, *85*, 977–1003. https://doi.org/10.1007/s11069-016-2615-3
Fernandez, A., Black, J., Jones, M., Wilson, L., & Salvador-carulla, L. (2015). Flooding and Mental Health : A Systematic Mapping Review. *PLOS ONE*, *10*, 1–20. https://doi.org/10.1371/journal.pone.0119929
Harto, S. B. (1993). *Analisis Hidrologi* (1st ed.). Penerbit Gramedia Pustaka Utama.
Hiệu, N., Hiếu, Đ. T., Bắc, Đ. K., & Phương, Đ. T. (2013). Assessment of Flood Hazard in Hanoi City. *VNU Journal of Earth and Environmental Sciences*, *29*, 26–37. https://js.vnu.edu.vn/EES/article/view/1562/1524
Hong, Y., Liu, L., Qiao, L., & Adhikari, P. (2014). Handbook Engineering Hydrology, Modeling,Climate Change, and Variability. In S. Eslamian (Ed.), *Climate Change and hydrological Hazards* (pp. 53–86). CRC Press.
Jenis dan Tarif atas Jenis Penerimaan Negera Bukan Pajak yang Berlaku Pada Badan Meteorologi, Klimatologi, dan Geofisika, (2018).
Islam, A. R. M. T. (2020). Flood susceptibility modelling using advanced ensemble machine learning models. *Geoscience Frontiers*, *12*(3). https://doi.org/10.1016/j.gsf.2020.09.006
Khattak, S. M., Anwar, F., Saeed, T. U., Sharif, M., Sheraz, K., & Ahmed, A. (2016). Floodplain Mapping Using HEC-RAS and ArcGIS : A Case Study of Kabul River. *Arabian Journal for Science and Engineering*, *41*, 1375–1390. https://doi.org/10.1007/s13369-015-1915-3
Meyerink, A, M. . (1970). *Chapter VII.3 ITC Textbook of Photo-Interpretation in hydrology, A Geomorpholoical Approach* (Netherlands (ed.)). ITC.
Ozkaya, A., & Akyurek, Z. (2019). Evaluating the use of bias-corrected radar rainfall data in three flood events in Samsun, Turkey. In *Natural Hazards* (Vol. 98, Issue 2). Springer Netherlands. https://doi.org/10.1007/s11069-019-03723-z
Parsa, A. S., Heydari, M., Sadeghian, M. S., & Moharrampour, M. (2013). Flood Zoning Simulation by HEC-RAS Model (Case Study: Johor River-Kota Tinggi Region). *Journal of River Engineering*, *1*, 29–34. http://www.scijour.com/page/article-frame.html?articleId=794
Prasad, R. N., & Pani, P. (2017). Geo-hydrological analysis and sub watershed prioritization for flash flood risk using weighted sum model and Snyder ' s synthetic unit hydrograph. *Modeling Earth Systems and Environment*, *3*, 1491–1502. https://doi.org/10.1007/s40808-017-0354-4
Pratiwi, A. N. & Santosa, P. B. (2021). Pemodelan Banjir dan Visualisasi Genangan Banjir untuk Mitigasi Bencana di Kali Kasin Kelurahan Bareng Kota Malang. *Journal of Geospatial Information Science and Engineering*, Vol. 4 No. 1 (2021). https://doi.org/10.22146/jgise.56525
Ramly, S., Tahir, W., Abdullah, J., Jani, J., Ramli, S., & Asmat, A. (2020). Flood Estimation for SMART Control Operation Using Integrated Radar Rainfall Input with the HEC-HMS Model. *Water Resources Management*, *34*(10), 3113–3127. https://doi.org/10.1007/s11269-020-02595-4
Sahid, S. (2024). Enhancing Digital Elevation Model Accuracy for Flood Modelling – A Case Study of the Ciberes River in Cirebon, Indonesia. *Forum Geografi*, *38*(1), 40–56. https://doi.org/10.23917/forgeo.v38i1.1839
Sahid, S., Ihsan, H. M., Saefulloh, M. A., & Ulhaq, W. D. (2024). Sensitivity Analysis of Digital Elevation Model in The Use of Hydrological Applications. *Rekayasa*, *17*(2), 306–319. https://doi.org/https://doi.org/10.21107/rekaya

sa.v17i2.22449
Sahid, S., Nurrohman, A. W., & Hadi, M. P. (2018). An investigation of Digital Elevation Model (DEM) structure influence on flood modelling. *International Conference on Environmental Resources Management in Global Region*, *148*, 1–12. https://doi.org/10.1088/1755-1315/148/1/012001
Santos, F. M. dos, Lollo, J. A. de, & Mauad, F. F. (2017). Estimating the surface runoff from natural environment data. *Management of Environment Quality: An International Journal*, *28*, 515–531. https://doi.org/10.1108/MEQ-07-2015-0137
Santosa, P. B., Mitani, Y. & Ikemi, H. (2010). Estimation of RUSLE EI30 based on 10 min interval rainfall data and GIS-based development of rainfall erosivity maps for Hitotsuse basin in Kyushu Japan. *18th International Conference on Geoinformatics*, Beijing, China, 2010, pp. 1-6, https://doi.org/10.1109/GEOINFORMATICS.2010.5568195
Sarido, L., Hardwinarto, S., & Aipassa, M. I. (2008). Debit Banjir Rancangan dan Kawasan Genangan. *Jurnal KehutananTropika Humida*, *1*, 35–48.
Sarkar, D., & Mondal, P. (2020). Flood vulnerability mapping using frequency ratio (FR) model: a case study on Kulik river basin, Indo-Bangladesh Barind region. *Applied Water Science*, *10*(1), 1–13. https://doi.org/10.1007/s13201-019-1102-x
Singh, B. K. (2014). Flood Hazard Mapping with Participatory GIS : The Case of Gorakhpur. *Environment and Urbanization ASIA*. https://doi.org/https://doi.org/10.1177/0975425314521546
Singh, P. K., Mishra, S. K., & Jain, M. K. (2014). A review of the synthetic unit hydrograph: from the empirical UH to advanced geomorphological methods. *Hydrological Sciences Journal*, *59*, 239–261. https://doi.org/10.1080/02626667.2013.870664
Snyder, F. F. (1938). Synthetic Unit Hydrographs. *Transactions American Geophysical Union*, *19*, 447–454. https://doi.org/10.1029/TR019i001p00447
Stephenson, J., Vaganay, M., Cameron, R., & Joseph, P. (2014). The long-term health impacts of repeated flood events. *WIT Transactions on Ecology and The Environment*, *184*, 201–212. https://doi.org/10.2495/FRIAR140171
Sushanth, K., & Bhardwaj, A. (2019). Assessment of landuse change impact on runoff and sediment yield of Patiala-Ki-Rao watershed in Shivalik foot-hills of northwest India. *Environmental Monitoring and Assessment*. https://doi.org/https://doi.org/10.1007/s10661-019-7932-z
Thapa, G., & Wijesekera, N. T. . (2017). Computation and Optimization of Snyder's Synthetic Unit Hydrograph Parameters. *UMCSAWM Water Conference*, *January*, 83–88.
Venus, D. K.-A. G. F. V. (2015). Modeling Flood Hazard Zones at the Sub-District Level with the Rational Model Integrated with GIS and Remote Sensing Approaches. *Water*, *7*. https://doi.org/https://doi.org/10.3390/w7073531
Vozinaki, A. K., Morianou, G. G., Alexakis, D. D., Tsanis, K., & Tsanis, I. K. (2017). Comparing 1D and combined 1D/2D hydraulic simulations using high-resolution topographic data: a case study of the Koiliaris basin, Greece. *Hydrological Sciences Journal*, *62*, 642–656. https://doi.org/10.1080/02626667.2016.1255746
Wilkerson, J., & Merwade, V. (2010). Determination of Unit Hydrograph Parameters for Indiana Watersheds. *Joint Transportation Research Program*, *September*, 114. https://doi.org/10.5703/1288284314266.This
Yucel, I. (2015). Assessment of a flash flood event using different precipitation datasets. *Natural Hazards*, *79*(3), 1889–1911. https://doi.org/10.1007/s11069-015-1938-9
Zope, P. E., Eldho, T. I., & Jothiprakash, V. (2016). Impacts of land use – land cover change and urbanization on flooding : A case study of Oshiwara River Basin in Mumbai , India. *Catena*, *145*, 142–154. https://doi.org/10.1016/j.catena.2016.06.009